ADVANCED FUNCTIONAL MATERIALS
www.afm-journal.de

www.MaterialsViews.com

Polyazines and Polyazomethines with Didodecylthiophene Units for Selective Dispersion of Semiconducting Single-Walled Carbon Nanotubes

*Widianta Gomulya, Vladimir Derenskyi, Erika Kozma, Mariacecilia Pasini, and Maria Antonietta Loi**

Polymer wrapped single-walled carbon nanotubes (SWNTs) have been demonstrated to be a very efficient technique to obtain high purity semiconducting SWNT solutions. However, the extraction yield of this technique is low compared to other techniques. Poly-alkyl-thiophenes have been reported to show higher extraction yield compare to polyfluorene derivatives. Here, the affinity for semiconducting SWNTs of two polymers with a backbone containing didodecylthiophene units interspersed with N atoms is reported. It is demonstrated that one of the polymers, namely, poly(2,5-dimethylidynenitrilo-3,4-didodecylthienylene) (PAMDD), has very high semiconducting SWNT extraction yield compared to the poly(3,4-didodecylthienylene)azine (PAZDD). The dissimilar wrapping efficiency of these two polymers for semiconducting SWNTs is attributed to the interplay between the affinity for the nitrogen atoms of the highly polarizable walls of SWNTs and the mechanical flexibility of the polymer backbones. Photoluminescence (PL) measurements demonstrate the presence of metallic tubes and SWNT bundles in the sample selected with PAZDD and higher purity of SWNT-PAMDD samples. The high purity of the semiconducting SWNTs selected by PAMDD is further demonstrated by the high performance of the solution-processed field-effect transistors (FETs) fabricated using a blade coating technique, which exhibit hole mobilities up to 33.3 $cm^2 V^{-1} s^{-1}$ with on/off ratios of 10^6.

1. Introduction

Single-walled carbon nanotubes (SWNTs) are promising nanomaterials for future electronic devices, such as transistors,[1] solar cells,[2] and bio/chemical sensors,[3] due to their high carrier mobility,[4] outstanding mechanical and chemical stabilities, and optical properties.[5] Because the electronic properties of nanotubes depend on their diameter and chirality, SWNTs may exhibit metallic or semiconducting properties. The main factor limiting their applicability in electronic devices is the mixture of metallic and semiconducting species in as-grown SWNTs. Several device applications, such as transistors, require high purity semiconducting SWNTs (s-SWNTs), while other applications, such as conductive electrodes, require enriched metallic SWNTs (m-SWNTs). Thus, post-growth purification is required to develop SWNT-based devices. In the last few years, many efforts have been devoted to separate s-SWNTs from metallic species.[6] Noncovalent functionalization has been widely investigated as a nondestructive purification process that can preserve the original electronic properties. These noncovalent methods rely on the wrapping of nanotubes with different molecules such as surfactants,[7,8] DNA,[9] and conjugated polymers.[10]

Sorting SWNTs by polymer wrapping is of particular interest compared to other similar techniques due to the high selectivity, easy availability of conjugated polymers and simple processing.[10] Although significant progress has been achieved in the study of conjugated polymers for sorting of semiconducting SWNTs, in the last few years the polymers used for sorting SWNTs have been limited to polythiophene,[11] polyfluorene,[10] and polycarbazole[12] derivatives. Polyfluorene derivatives are known to allow effective selection of mainly near armchair SWNTs,[10] however, the extraction yield is generally very low, which hinders the mass production of s-SWNTs. Recently, it has been reported that the concentration yield can be improved by increasing the length of alkyl side chains, which allow a better interaction of the polymer chain with the SWNT walls;[13] or by performing multiple extraction steps.[14] Polythiophenes instead are less selective,[11] but can provide a much higher extraction yield (≈180 μg mL^{-1}), which is more than seven times higher compared to polyfluorene derivatives with the same alkyl side chain length. To date, poly-alkylthiophenes have been reported to show the highest extraction yield of s-SWNTs. The efficient selection of s-SWNTs with high purity and concentration is a fundamental requirement to achieve in future mass production of SWNT-based electronic devices.

W. Gomulya, V. Derenskyi, Prof. M. A. Loi
Zernike Institute for Advanced Materials
University of Groningen
Nijenborgh 4, Groningen 9747, AG
The Netherlands
E-mail: m.a.loi@rug.nl
Dr. E. Kozma, Dr. M. Pasini
Istituto per lo Studio delle Macromolecole (CNR)
Via E. Bassini 15, 20133 Milano, Italy

DOI: 10.1002/adfm.201502912

It is worthy to note that up until now the main backbone of the conjugated polymers able to wrap SWNTs was principally composed by carbon, or sulfur, and nitrogen atoms inserted in the aromatic moieties like thiophene and carbazole.[12] The direct introduction of heteroatoms with coordinative properties like nitrogen in the semiconducting backbone is expected to change the interaction with SWNTs, giving new information on the polymer-wrapping selection mechanism and opening the way to new tailored materials with improved properties.

In this context, this work reports the first use of conjugated polyazines and polyazomethines with thienylene units and hydrocarbon side chains to selectively disperse semiconducting SWNTs.[15] Poly(2,5-dimethylidynenitrilo-3,4-didodecylthienylene) (PAMDD) shows a very high extraction yield (up to 180 μg mL^{-1}), which is similar to poly(3-dodecylthiophene-2,5-diyl) (P3DDT), while poly(3,4-didodecylthienylene)azine (PAZDD) has lower selectivity. The dissimilar wrapping efficiency of these two polymers for semiconducting SWNTs is attributed to the interplay between the affinity for the nitrogen atoms of the highly polarizable walls of SWNTs and the mechanical flexibility of the polymer backbones. Both effects are lowered in PAMDD by the insertion of an extra phenyl ring, resulting in a lower affinity for highly polarizable species (metallic tubes) and higher interaction with smaller diameter semiconducting SWNTs, which are selected with higher concentration. While in PAZDD the conjugated diimine ligand —C=N—N=C—, the versatile coordination properties,[16] and the higher backbone flexibility results in a large number of metallic tubes, and a much lower yield for semiconducting tubes. PL measurements demonstrate the presence of metallic tubes and bundles in the sample selected with PAZDD and the high purity of the PAMDD samples. The high purity and concentration of the semiconducting SWNTs selected by PAMDD are further demonstrated by the fabrication of field effect transistors by blade coating method showing hole mobility up to 33.3 $cm^2 V^{-1} s^{-1}$ and an on/off ratio of 10^6.

2. Results and Discussion

Polyazomethine and polyazine are known to have third-order nonlinear optical properties, which have been widely used for waveguides.[17] They are environmentally stable, easy to prepare, and have good thermal stability. The chemical structures of the two polymers investigated in this work are shown in the insets of **Figure 1**a. The HOMO/LUMO levels are −5.9/−3.42 and −6.2/−3.93 eV for PAMDD and PAZDD, respectively (see Supporting Information). Both polymers contain didodecylthiophene units interspersed with nitrogen atoms in their backbones, and the only difference is the presence of the benzene ring between the two nitrogen atoms in PAMDD, resulting in dissimilar polymer backbone planarity.[15] The extra aromatic ring makes PAMDD less planar and also gives it a higher band gap than PAZDD. Figure S1 (Supporting Information) displays the absorption and PL of the two polymers in solution. The absorption of both systems ranges from 350 to 600 nm with the maxima at 475 nm for PAMDD, and at 513 nm for PAZDD, corresponding to the absorption of the lowest energy π–π^* transition of the aromatic ring.[15]

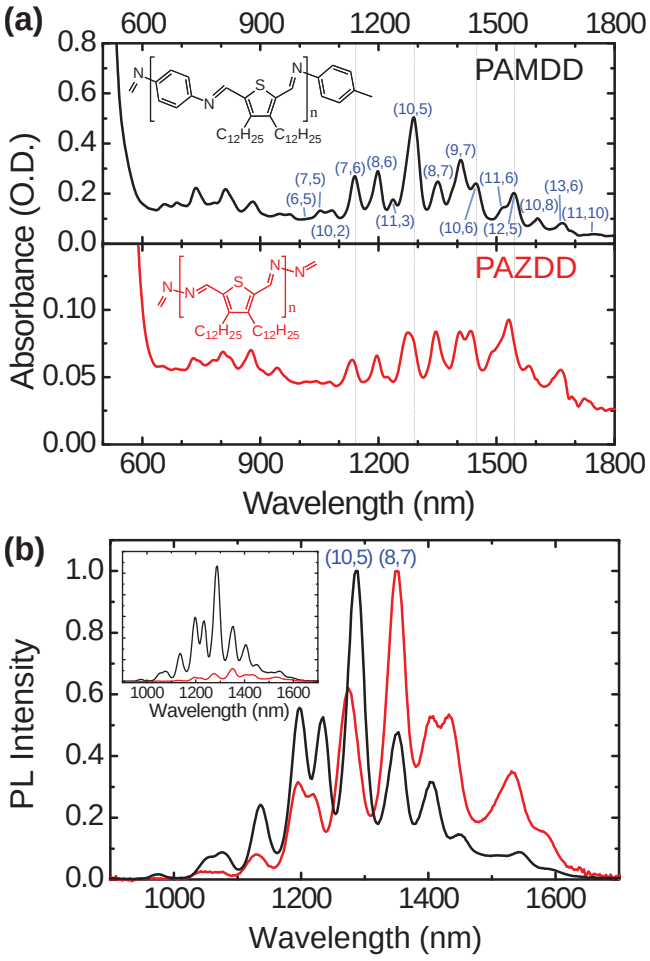

Figure 1. a) Absorbance of PAMDD- and PAZDD-wrapped SWNT solutions with the assignment of the SWNT chiralities. The chemical structures of the polymers are shown as insets. b) Normalized photoluminescence (PL) spectra of the solutions as in (a); inset: same PL spectra as in (b) before normalization.

Figure 1a reports the absorption spectra of the SWNT dispersions obtained with the two polymers using a nanotube to polymer weight ratio 1:2. The SWNT species (as indicated in the top figure) were assigned using the semiempirical formula[18]

$$E_{11} = \frac{1241}{A_1 + A_2 d} + A_3 \frac{\cos 3\theta}{d^2}$$

where E_{11} is the first electronic transition, d is the diameter, and θ is the chiral angle of the corresponding SWNT species. A_1, A_2, and A_3 are scaling parameters fitted from the experimental data. The values of the fitted parameters are listed in Table S1 (Supporting Information). The two polymers select the same SWNT chiralities even though with dissimilar proportion of the different species and a small shift in the peak position, which will be discussed in the following.

From the absorption spectra, it is evident that with respect to PAZDD, PAMDD selects a larger amount of smaller diameter SWNTs. We can qualitatively explain this behavior as being caused by the fact that PAZDD has a more flexible

backbone than PAMDD.[15] A more flexible backbone allows a larger number of conformations, which makes the interaction with a larger number of different kinds of SWNT species possible. As previously mentioned, the phenyl rings in the PAMDD make the backbone stiffer, limiting the conformation of the polymer chain and favoring higher interaction with certain SWNTs, thanks to the increased π–π stacking.

After having investigated the difference in SWNT selectivity of PAMDD and PAZDD, it is next important to compare this new polymers with previosly reported ones. To do so, we estimated the SWNT concentration by taking into account the absorption cross section ($\alpha(E_{11}^{S}) \approx 1 \times 10^{-18}$ atom^{-1}) of individually dispersed nanotubes obtaining concentration of ≈180 and ≈25 μg mL^{-1} for PAMDD-SWNTs and PAZDD-SWNTs, respectively.[19] It is interesting to notice that the concentration of SWNTs selected by PAMDD is comparable to the one obtained by P3DDT with the same conditions, while the concentration selected by PAZDD is in the range of the one obtained by poly(9,9-di-*n*-dodecylfluorene-2,7-diyl) (PF12) (see Figure S2 in the Supporting Information). Overall, PAMDD selects s-SWNTs more than seven times more effectively than PAZDD. Interestingly, if we consider the extraction capability of poly(9,9-di-*n*-octylfluorene-2,7-diyl) (PFO), poly(9,9-dioctylfluorene-alt-benzothiadiazole) (F8BT), and poly(9,9-dioctylfluorene-alt-pyridine) (PFO-py), it is noticeable that the polymers with a stiffer backbone (i.e., those with higher number of aromatic rings), namely, F8BT and PFO-py, are able to sort more specific nanotube populations.[20,21] Importantly, in the absorption spectrum of the PAZDD-SWNT dispersion, a higher background is observed. This is a strong indication that this SWNT dispersion contains metallic tubes or small nanotube bundles.[22]

As already reported before, nitrogen atoms have strong adsorption to metallic surfaces due to their electron-rich nature.[23] A practical example of the interaction with SWNTs is provided by self-assembled monolayer containing nitrogen which have been proposed and used intensively as a method to adsorb a higher number of SWNTs on substrates.[11,24] Therefore, the effective interaction of nitrogen electron-rich systems with highly polarizable objects can explain both the high yield of semiconducting SWNTs obtained with PAMDD and the appearance of metallic tubes in the PAZDD dispersion. In the case of PAZDD, the possibility of donating 2 to 8 electrons through the C=N group and the nitrogen lone pair[25] makes interaction with metallic tubes highly favorable. While in the case of PAMDD, the presence of a phenyl ring interplayed between the C=N group makes the interaction with metallic species more difficult.

Figure 1a shows a clear shift between the absorption features of the same SWNTs selected by the two polymers (see gray dashed lines in the figure). This effect is generally ascribed to dissimilar effective dielectric constant of the medium (solvatochromism). However, solvatochromism in systems which use the same solvent is smaller than in this case, where the difference in the same E_{11} transition of the samples is in the order of 20–35 meV (see Figure S3 in the Supporting Information).[26,27] This large effect can be ascribed either to a different dielectric constant of the two polymers, or to a dissimilar coverage of the SWNT walls in the two cases, which tunes the contact with toluene (ε toluene 2.4). From impedance measurements, we obtained static dielectric constants of 2.3 and 2.2 for PAMDD and PAZDD, respectively. This minor difference in the dielectric constants cannot explain the experimental shift of the absorption peaks. A dissimilar coverage of the SWNT walls could be justified by the fact that the phenyl rings in the PAMDD polymer are not coplanar with the N—N bonds,[28] thus resulting in a different local dielectric constant. However, this explanation considering the dielectric constant of toluene seems rather improbable. A further possible explanation is an electronic interaction between the polymer chains and the SWNTs; for example, interaction involving charge transfer has been reported to generate a redshift of the SWNT absorption peaks.[29] Also, the formation of small bundles of semiconducting and metallic tubes can be a very plausible explanation, since metallic species have an influence on the local screening of the excitation.

The PL spectra of the nanotubes dispersed with the two polymers are shown in Figure 1b. While the PL spectra of SWNT-PAMDD show similar peak-to-peak ratio to the absorption spectra, indicating a good SWNT individualization; the SWNT-PAZDD PL shows a very dissimilar intensity distribution with respect to the absorption, which we attribute to a strong energy transfer between adjacent tubes. In agreement with this observation, the PL quantum yield estimated for the SWNT-PAZDD dispersion is about 1 order of magnitude lower compared to the one of the SWNT-PAMDD dispersion (Figure S4, Supporting Information), confirming the presence of small bundles in the PAZDD dispersed samples.[30]

PL lifetime measurements can help to clarify the formation of bundles and the presence of metallic tubes. The PAMDD-dispersed SWNTs show a bi-exponential decay time with components of 6 and 29 ps (**Figure 2**a,c), which is similar to the exciton lifetime previously reported for SWNT-P3DDT.[31] Instead, for SWNTs selected with PAZDD (Figure 2b,d) the lifetime is extremely fast and appears limited by the time resolution of the experimental setup (2 ps). This is a further strong indication of the fact that PAZDD favors the formation of SWNTs bundles involving metallic species.

In order to remove the excess polymer in the dispersions, and at the same time to increase the SWNT concentration, we performed a second ultracentrifugation following the method we have previously reported.[24] The absorption spectra of the samples after the excess polymer removal are shown in **Figure 3**a. Both solutions show a reduced polymer absorption peak (475 nm and 513 nm), showing the effectiveness of the procedure.[31] The PL spectra of the corresponding enriched solutions are shown in Figure 3b. Interestingly, even though the absorption before (dashed line) and after (solid line) second centrifugation (Figure 3a) shows similar SWNTs population and relative intensity of the SWNT species, the PL spectra before and after enrichment (Figure 3b) are very different.

Two main features can be observed in the PL spectra. First, the SWNT-PAMDD after enrichment shows a redistribution of the PL intensity. Since no change is observed in the absorption spectrum, the redistribution of intensity is the result of an energy transfer from large band gap to smaller band gap SWNTs. Probably, after the removal of the excess polymer, the polymer chains present are insufficient to stabilize the individual tubes causing formation of small bundles. Second,

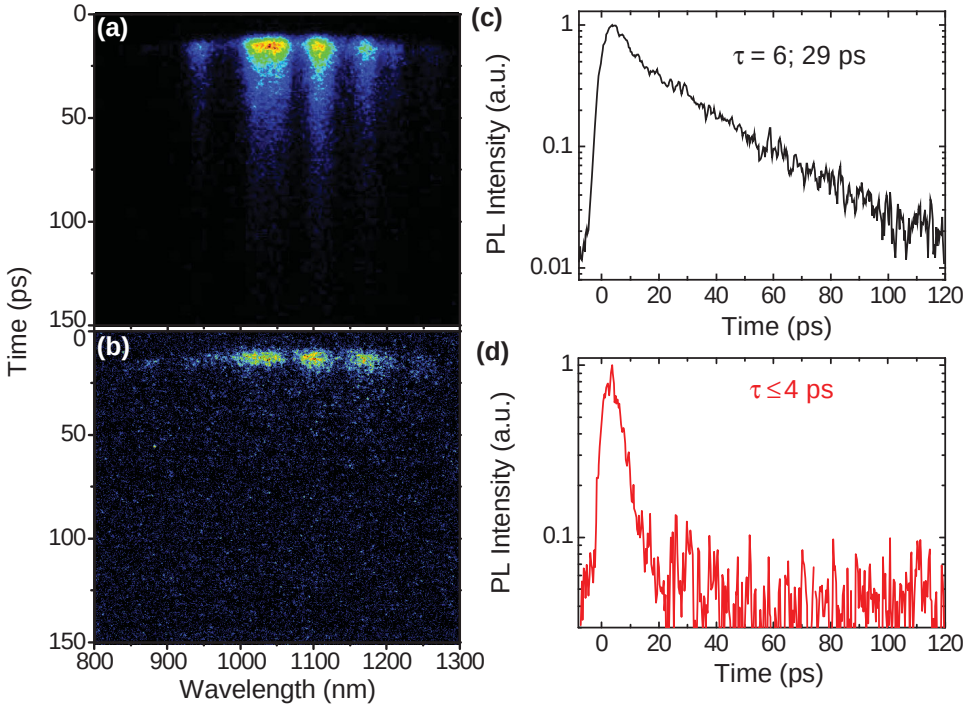

Figure 2. Time-resolved photoluminescence of a) PAMDD- and b) PAZDD-wrapped SWNTs. Decay dynamics of the (7,5) tubes wrapped by c) PAMDD and d) PAZDD.

the PL of the SWNT-PAZDD (Figure 3b) enriched sample (red solid line) is much weaker compared to the one before enrichment (red dashed line). Also, in this case a stronger tendency of the SWNT to re-aggregate and form bundles when the excess polymer is removed appears. Furthermore, for this sample, the appearance of the metallic tubes in the bundles have strong consequences such as lowering the PL quantum yield.

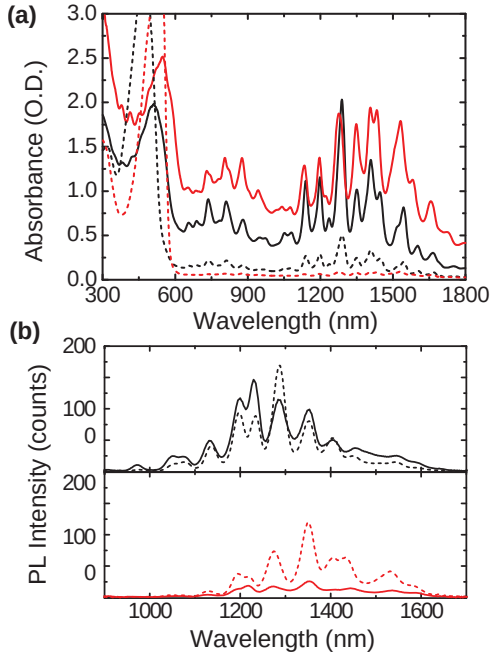

Figure 3. a) Absorption and b) photoluminescence spectra of SWNT-PAMDD (black) and SWNT-PAZDD (red) dispersions before (dashed line) and after (solid line) excess polymer removal.

Time-resolved PL measurements of SWNT-PAMDD before and after enrichment are shown in Figure S5 (Supporting Information). The lifetime of the SWNT-PAMDD sample after enrichment is slightly shorter (τ_1 = 6 ps, τ_2 = 23 ps) than the one before enrichment (τ_1 = 6 ps, τ_2 = 29 ps). This result is in agreement with our hypothesis of formation of small bundles in which energy transfer from the larger to the smaller band gap tube occurs. In the case of the SWNT-PAZDD, the lifetime was already very short (limited by the instrumental resolution) and stayed below that after enrichment, confirming the presence of metallic tubes in the selected small bundles.

To demonstrate the quality of the semiconducting SWNTs obtained in this way, we utilize the inks for the fabrication of bottom gate/bottom-contact field effect transistors following previously reported procedures.[24,32] For comparison purpose, the concentrations of the two samples (PAMDD-based and PAZDD-based) were adjusted to the same value, this means a dilution for the high-yield PAMDD-based sample. Both pristine and enriched SWNT solutions were deposited by blade coating to obtain a network of semialigned SWNT in the channel. Recently, using this technique we have reported better device performances, compared to the devices fabricated by drop-casting.[32]

The output curves of the FETs fabricated with both SWNT samples before enrichment are shown in Figure S6 (Supporting Information). The output I_{DS}–V_{DS} curves show good saturation current in the hole accumulation regime. The SWNT-PAMDD FETs show an average on/off ratio as high as

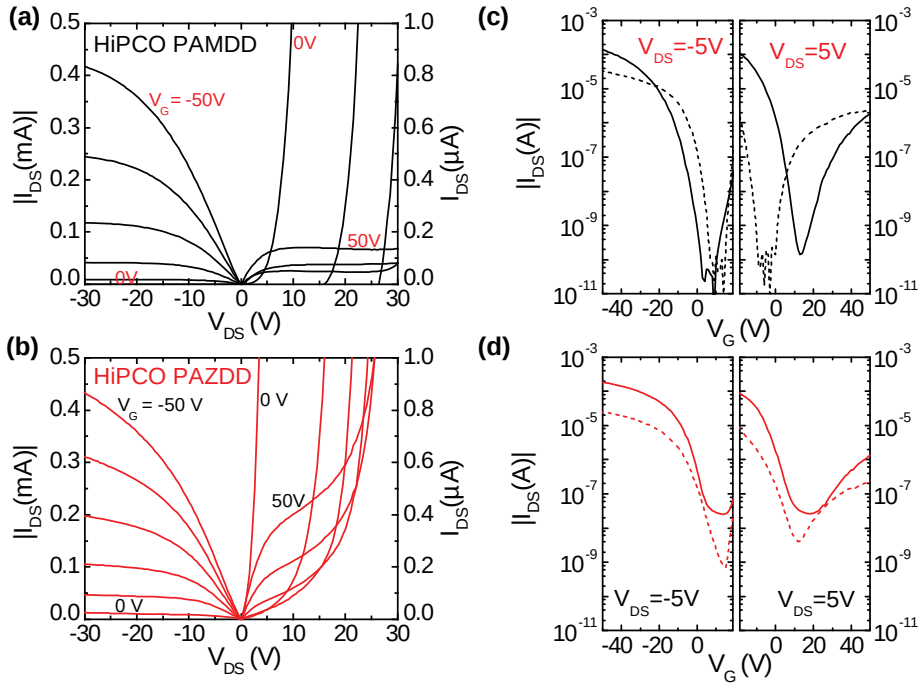

Figure 4. Output characteristics of SWNT FETs dispersed with a) PAMDD and b) PAZDD after enrichment. c,d) Transfer characteristics for hole and electron channel before (dashed line) and after (solid line) enrichment.

10^6 for hole current at V_{DS} = −5 V (**Figure 4**c; dashed lines); while SWNT-PAZDD FETs show more than 1 order of magnitude lower on/off ratio, mainly due to the higher off current as shown in Figure 4d (dashed line). The higher off current obtained in this case, is an additional evidence of the presence of metallic tubes in the sample. It is important to underline that the FET structure investigated has channel length of 20 μm and channel width of 10 mm. The relatively short channel length is fundamental to verify the presence of metallic tubes in the inks.[33]

Interestingly, all devices are dominated by hole current even if they have been measured in inert atmosphere. In this respect, they are similar to SWNT-P3DDT-based devices, where we have reported the trapping of electrons due to the polymer.[32] The hole mobility calculated from the linear operational regime of the FET transfer curves are 0.54 $cm^2\ V^{-1}\ s^{-1}$ and 0.18 $cm^2\ V^{-1}\ s^{-1}$ for PAMDD- and PAZDD-wrapped SWNTs, respectively. The mobility obtained from the SWNT-PAMDD devices is comparable to the one obtained with P3DDT-SWNTs under similar conditions.[32]

After the enrichment, the devices show increased performance both in the hole and electron accumulation regime as shown in Figure 4a,b. The hole current increases by 30 times with respect to the devices fabricated with nonenriched dispersions, while an electron current in the order of sub-micro Ampere is measured. After enrichment, ohmic contact for hole injection can be achieved, especially for SWNT-PAMDD devices. The better contact and higher saturation current point to the effectiveness of the polymer removal, which reduces the Schottky barrier between the gold electrodes and the nanotubes, and also lowers the barrier between SWNTs in the networks.

The transfer curves of the devices after polymer removal are shown in Figure 4c,d (solid lines). The off-current of the PAMDD-SWNTs devices remains constant, while that of SWNT-PAZDD increases. This higher off current is due to an increased percolation between metallic SWNTs in the transistor channel.[34] The hole mobility after the enrichment improves by nearly a factor of three from 0.54 to 1.47 $cm^2\ V^{-1}\ s^{-1}$ for SWNT-PAMDD, and 1 order of magnitude from 0.18 to 1.24 $cm^2\ V^{-1}\ s^{-1}$ for SWNT-PAZDD. Again, the increase in mobility is mainly due to the lower amount of free polymer, which allows a better interconnection between the SWNT network.

Surprisingly, the devices before enrichment show lower subthreshold swings compared to those after enrichment. The difference in the subthreshold swings is more obvious for the electron channel, which goes from SS = 2.8 to 6.2 V dec^{-1} for SWNT-PAMDD, and from SS = 13.5 to 18 V dec^{-1} for SWNT-PAZDD. The lower subthreshold swing corresponds to a reduced trap density in the channels. The traps are most probably located at the interface between the SiO_2 substrate and the SWNT network. Since no surface treatment on the SiO_2 substrate was performed to passivate OH groups, we suppose that the excess polymer may have a role in passivating those surface states. This charge trapping is also observed by extracting the values of threshold voltage of the carrier accumulation of the devices before and after enrichment (Figure S7, Supporting Information). The threshold voltage for hole accumulation is found to have very small shift before and after enrichment. While for the electron accumulation, after the enrichment, the threshold voltage shifts toward positive voltages: ΔV_{Th} = +25 V and +11 V for PAMDD and PAZDD, respectively. The positive threshold voltage shift was observed in previous reports and is due to a higher amount of electron traps.[24]

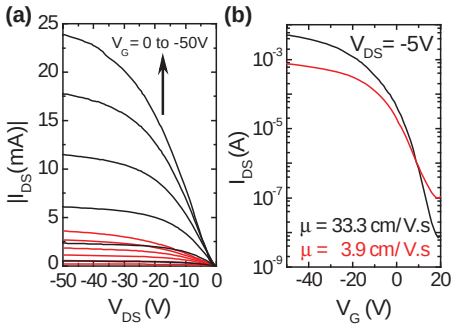

Figure 5. a) Output and b) transfer characteristics of the FET devices fabricated with high-concentration (≈700 μg mL^{-1}) SWNT-PAMDD (black) and SWNT-PAZDD (red).

For high-quality semiconducting SWNT solutions, a linear relation between the concentration of the SWNTs and the on-current of the transistor is expected; we therefore increased the concentration of the SWNTs in the inks (700 μg mL^{-1}; four times more concentrated than reported in Figure 1a). With these concentrated solutions, very dense and homogeneous nanotube networks are obtained by blade coating. Figure S8 (Supporting Information) shows an example of the atomic force microscopy (AFM) images obtained analyzing the deposited network in different regions of the substrate.

Figure 5a shows output characteristics of the FETs. The devices show on-current up to 25 mA, which corresponds to a current density of 25 mA mm^{-1}, which are much higher than that previously reported in the devices fabricated by SWNT obtained using a similar technique (SWNT-P3DDT) with a 10 mm channel width.[11,32] In Figure 5b, the transfer characteristics of the devices fabricated on a 1 mm channel width with s-SWNT inks are shown. The smaller channel width (1 mm) was chosen because of the enormous output current, exceeding our instrumentation limit, obtained in devices with longer channel width.[13,24,32] The linear mobility for the SWNT-PAMDD device is 33.3 cm^2 V^{-1} s^{-1}, while for SWNT-PAZDD it is 3.9 cm^2 V^{-1} s^{-1}. The PAMDD device together with the high mobility displays an on/off ratio of 10^6, which is record performance for FETs fabricated by solution processable small diameter (≈1 nm) semialigned/random network of SWNTs.

This outstanding result is derived from the high concentration (700 μg mL^{-1}) of the solution used, only achievable with very high yield extraction systems as the PAMDD and with the high purity of the semiconducting nanotube ink. Importantly, the PAMDD-based samples have been used for the fabrication of single-SWNT FETs with a channel length of 300 nm, leading to semiconducting SWNTs purity estimation superior to 99.9%.[35]

3. Conclusion

In conclusion, polyazines and polyazomethines with didodecylthiophene are demonstrated to be capable of selectively dispersing semiconducting SWNTs. By comparing two similar conjugated polymers, we have obtained new information on the polymer-wrapping selection mechanism and on the design rules for the polymer. Both of these polymers contains C=N group in the main chain = which is isoelectronic with the C=C linkage, assuring the semiconducting properties of the backbone, but with higher coordinative properties due to the different electronegativity of nitrogen and the presence of lone pairs increasing the affinity for the polarizable walls of the carbon nanotubes. PAZDD shows higher interaction with metallic species and with SWNT of wider diameter due to the coordinative properties of the —C=N—N=C— linkage in the backbone and its flexibility. PL quantum yield, time-resolved PL measurements, and SWNT FET devices all point to the fact that PAZDD dispersion contains more bundles and a nonzero concentration of metallic SWNTs. PAMDD demonstrates higher extraction yield for semiconducting SWNTs compared to PAZDD, which we attribute to the mitigation of the nitrogen effect by the presence of the phenyl ring in the backbone. SWNT FETs fabricated from SWNT-PAMDD dispersions show very high current compared to other reported polymer-wrapped SWNT FETs with hole mobility up to 33.3 cm^2 V^{-1} s^{-1} and an on/off ratio of 10^6. The finding of this new conjugated polymer to select high-concentration (up to 180 μg mL^{-1}) SWNTs with high purity opens the possibility for scaling up the separation of s-SWNTs by polymer wrapping methods for large-scale high-performance electronic device applications.

4. Experimental Section

Preparation and Characterization of the Semiconducting SWNT Dispersion: PAMDD and PAZDD were synthesized as described previously.[15] The molecular weights of the batch used are M_w 67 400, M_w/M_n 1.93 and M_w 16 300, M_w/M_n = 1.67 for PAMDD and PAZDD, respectively. HiPCO SWNTs were purchased from Unidym Inc. To prepare the sorted s-SWNT solution, first 6 mg of polymer were fully dissolved in 10 mL toluene, and afterward 3 mg of SWNTs were mixed in the solution. The sample was sonicated for 2 h at 16 °C with a cup-horn sonicator (Misonix 3000, output power 65 W) and afterward ultracentrifuged for 1 h at 40,000 rpm (196 000*g*) (Beckman Coulter Optima XE-90; rotor: SW55Ti). After ultracentrifugation, the supernatant was carefully separated for all the experiments conducted at low concentration. A second ultracentrifugation (5 h at 55,000 rpm (367 000*g*)) was performed in order to remove excess polymer and to increase the SWNTs concentration. Here, the supernatant was discarded, and the precipitate (pellet) containing the enriched SWNTs was redispersed in the desired solvent quantity. Absorption spectra were recorded by a UV–Vis–NIR spectrophotometer (Shimadzu UV-3600) in the range from 300 to 1800 nm.

Photoluminescence Measurements: PL measurements were performed by exciting the samples at 800 nm with a Kerr mode-locked Ti-Sapphire laser, delivering 150 fs pulses with a repetition frequency of 76 MHz. Steady-state PL spectra were measured by an InGaAs photodetector array from Andor, while the time-resolved PL measurements were recorded by a streak camera with a NIR-sensitive photocathode (Hamamatsu Photonics) working in synchroscan mode (time resolution around 2 ps). All spectra were corrected for instrumental response.

Device Fabrication and Characterization: The prepared semiconducting SWNT dispersions were deposited on top of highly doped silicon substrate with 230 nm of SiO_2 layer. The substrates were lithographically pre-patterned with electrodes made with 10 nm of Ti and 30 nm of Au, defining a channel length of 20 μm and channel width of 10 and 1 mm. The deposition of the active materials was performed by blade coating (ZAA 2300 automatic film applicator coater, Zehntner, Sissach, Switzerland) in order to align SWNTs along one direction.[32] After the deposition, the substrates were annealed for 1 h at 120 °C to remove

residual solvent. The electrical measurements were performed using a probe station connected to a semiconductor parameter analyzer (Agilent E5262A). All fabrication and characterization procedures were done in a nitrogen-filled glovebox.

Supporting Information

Supporting Information is available from the Wiley Online Library or from the author.

Acknowledgements

This research was funded by Stichting voor Technische Wetenschappen (STW, Utrecht, The Netherlands). W.G. gratefully acknowledges University of Groningen for the Bernoulli scholarship. The authors would like to acknowledge J. M. S. Rios, L. H. Lai, M. I. Nugraha, M. T. Abdu-Aguye for discussions, and A. F. Kamp for the technical support.

Received: July 14, 2015
Published online: August 17, 2015

[1] R. Martel, T. Schmidt, H. R. Shea, T. Hertel, P. Avouris, *Appl. Phys. Lett.* **1998**, *73*, 2447.
[2] D. J. Bindl, A. S. Brewer, M. S. Arnold, *Nano Res.* **2011**, *4*, 1174.
[3] E. S. Snow, F. K. Perkins, E. J. Houser, S. C. Badescu, T. L. Reinecke, *Science* **2005**, *307*, 1942.
[4] T. Dürkop, S. A. Getty, E. Cobas, M. S. Fuhrer, *Nano Lett.* **2004**, *4*, 35.
[5] P. Avouris, J. Appenzeller, R. Martel, S. J. Wind, *Proc. IEEE* **2003**, *91*, 1772.
[6] M. C. Hersam, *Nat. Nanotechnol.* **2008**, *3*, 387.
[7] M. J. O'Connell, S. M. Bachilo, C. B. Huffman, V. C. Moore, M. S. Strano, E. H. Haroz, K. L. Rialon, P. J. Boul, W. H. Noon, C. Kittrell, J. Ma, R. H. Hauge, R. B. Weisman, R. E. Smalley, *Science* **2002**, *297*, 593.
[8] M. S. Arnold, A. A. Green, J. F. Hulvat, S. I. Stupp, M. C. Hersam, *Nat. Nanotechnol.* **2006**, *1*, 60.
[9] M. Zheng, A. Jagota, M. S. Strano, A. P. Santos, P. Barone, S. G. Chou, B. A. Diner, M. S. Dresselhaus, R. S. Mclean, G. B. Onoa, G. G. Samsonidze, E. D. Semke, M. Usrey, D. J. Walls, *Science* **2003**, *302*, 1545.
[10] A. Nish, J.-Y. Hwang, J. Doig, R. J. Nicholas, *Nat. Nanotechnol.* **2007**, *2*, 640.
[11] H. W. Lee, Y. Yoon, S. Park, J. H. Oh, S. Hong, L. S. Liyanage, H. Wang, S. Morishita, N. Patil, Y. J. Park, J. J. Park, A. Spakowitz, G. Galli, F. Gygi, P. H.-S. Wong, J. B.-H. Tok, J. M. Kim, Z. Bao, *Nat. Commun.* **2011**, *2*, 541.
[12] F. Lemasson, N. Berton, J. Tittmann, F. Hennrich, M. M. Kappes, M. Mayor, *Macromolecules* **2011**, *45*, 713.
[13] W. Gomulya, G. D. Costanzo, E. J. F. de Carvalho, S. Z. Bisri, V. Derenskyi, M. Fritsch, N. Fröhlich, S. Allard, P. Gordiichuk, A. Herrmann, S. J. Marrink, M. C. dos Santos, U. Scherf, M. A. Loi, *Adv. Mater.* **2013**, *25*, 2948.
[14] J. Ding, Z. Li, J. Lefebvre, F. Cheng, G. Dubey, S. Zou, P. Finnie, A. Hrdina, L. Scoles, G. P. Lopinski, C. T. Kingston, B. Simard, P. R. L. Malenfant, *Nanoscale* **2014**, *6*, 2328.
[15] S. Destri, M. Pasini, C. Pelizzi, W. Porzio, G. Predieri, C. Vignali, *Macromolecules* **1999**, *32*, 353.
[16] H. S. Huh, S. H. Kim, S. Y. Yun, S. W. Lee, *Polyhedron* **2008**, *27*, 1229.
[17] S. Destri, M. Pasini, W. Porzio, A. Zappettini, F. D'Amore, *J. Opt. Soc. Am. B* **2007**, *24*, 1505.
[18] J. H. Choi, M. S. Strano, *Appl. Phys. Lett.* **2007**, *90*, 223114.
[19] N. Stürzl, F. Hennrich, S. Lebedkin, M. M. Kappes, *J. Phys. Chem. C* **2009**, *113*, 14628.
[20] M. Tange, T. Okazaki, S. Iijima, *J. Am. Chem. Soc.* **2011**, *133*, 11908.
[21] M. Tange, T. Okazaki, S. Iijima, *Nanoscale* **2013**, 6, 248.
[22] A. V. Naumov, S. Ghosh, D. A. Tsyboulski, S. M. Bachilo, R. B. Weisman, *ACS Nano* **2011**, *5*, 1639.
[23] E. Greenhalgh, N. Slack, B. M. W. Trapnell, *Trans. Faraday Soc.* **1956**, *52*, 865.
[24] S. Z. Bisri, J. Gao, V. Derenskyi, W. Gomulya, I. Iezhokin, P. Gordiichuk, A. Herrmann, M. A. Loi, *Adv. Mater.* **2012**, *24*, 6147.
[25] C.-J. Lin, W.-S. Hwang, M. Y. Chiang, *J. Organomet. Chem.* **2001**, *640*, 85.
[26] J. Gao, W. Gomulya, M. A. Loi, *Chem. Phys.* **2013**, *413*, 35.
[27] C. A. Silvera-Batista, R. K. Wang, P. Weinberg, K. J. Ziegler, *Phys. Chem. Chem. Phys.* **2010**, *12*, 6990.
[28] C.-J. Yang, S. A. Jenekhe, *Macromolecules* **1995**, *28*, 1180.
[29] O. Kiowski, S. Lebedkin, F. Hennrich, S. Malik, H. Rösner, K. Arnold, C. Sürgers, M. M. Kappes, *Phys. Rev. B* **2007**, *75*, 075421.
[30] T. Koyama, K. Asaka, N. Hikosaka, H. Kishida, Y. Saito, A. Nakamura, *J. Phys. Chem. Lett.* **2011**, *2*, 127.
[31] W. Gomulya, J. M. Salazar Rios, V. Derenskyi, S. Z. Bisri, S. Jung, M. Fritsch, S. Allard, U. Scherf, M. C. dos Santos, M. A. Loi, *Carbon* **2015**, *84*, 66.
[32] V. Derenskyi, W. Gomulya, J. M. S. Rios, M. Fritsch, N. Fröhlich, S. Jung, S. Allard, S. Z. Bisri, P. Gordiichuk, A. Herrmann, U. Scherf, M. A. Loi, *Adv. Mater.* **2014**, *26*, 5969.
[33] S. Park, H. W. Lee, H. Wang, S. Selvarasah, M. R. Dokmeci, Y. J. Park, S. N. Cha, J. M. Kim, Z. Bao, *ACS Nano* **2012**, *6*, 2487.
[34] C. W. Lee, C.-H. Weng, L. Wei, Y. Chen, M. B. Chan-Park, C.-H. Tsai, K.-C. Leou, C. H. P. Poa, J. Wang, L.-J. Li, *J. Phys. Chem. C* **2008**, *112*, 12089.
[35] V. Derenskyi, W. Gomulya, E. Kozma, M. Pasini, M. A. Loi, unpublished.